RESEARCH ARTICLE | MAY 24 2024

High-resolution ghost imaging through dynamic and complex scattering media with adaptive moving average correction

Qian Song ; Qing Huo Liu ; Wen Chen

Appl. Phys. Lett. 124, 211104 (2024)
https://doi.org/10.1063/5.0211930

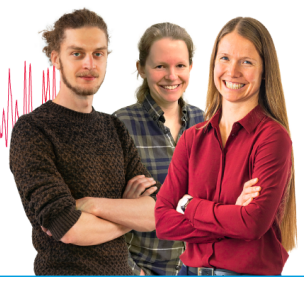

Applied Physics Letters ARTICLE pubs.aip.org/aip/apl

High-resolution ghost imaging through dynamic and complex scattering media with adaptive moving average correction

Cite as: Appl. Phys. Lett. **124**, 211104 (2024); doi: 10.1063/5.0211930
Submitted: 2 April 2024 · Accepted: 14 May 2024 ·
Published Online: 24 May 2024

Qian Song,[1,2] Qing Huo Liu,[2,a)] and Wen Chen[1,a)]

AFFILIATIONS

[1]Department of Electrical and Electronic Engineering & Photonics Research Institute, The Hong Kong Polytechnic University, Hong Kong, China
[2]Eastern Institute of Technology, Ningbo, China

[a)]**Authors to whom correspondence should be addressed:** qhliu@eitech.edu.cn and owen.chen@polyu.edu.hk

ABSTRACT

Optical imaging through dynamic and complex scattering media has attracted various applications, e.g., ranging from scene imaging to cell imaging. Nevertheless, imaging through complex media is full of challenges attributed to the inhomogeneous scattering, leading to nonlinear effects. Although ghost imaging (GI) has proven effective in solving some scattering problems, dynamic and complex scattering still requires an efficient solution. In this Letter, we report a model based on adaptive moving average (AMA) to correct the influence of dynamic scattering media from a statistical perspective for high-resolution GI. The developed AMA correction method selects an appropriate time window based on the changing trend of measured single-pixel light intensities to accurately correct a series of dynamic scaling factors. Then, the corrected single-pixel light intensities are used for ghost reconstruction using a second-order correlation algorithm. A series of optical experiments are conducted to verify superiority of the proposed method. Moreover, the proposed method can be applied with other algorithms to enhance the quality of the reconstructed ghost images. By leveraging a statistical model based on the measured data, the proposed scheme offers an enhanced solution to solving dynamic and complex scattering problems in GI.

Optical imaging has attracted numerous applications in scattering media, e.g., ocean monitoring,[1,2] imaging in foggy environments,[3,4] and biological imaging.[5–7] Optical imaging usually relies on rectilinear beam propagation and minimal volumetric attenuation to capture an object or its location in real-world scenes via radiation beams detected by a sensor, e.g., charge-coupled device (CCD). However, the presence of a complex scattering medium in the wave propagation path, e.g., severe weather, turbid water, or thick biological tissue, severely compromises an ideal or effective imaging. The absorption and scattering properties of light caused by scattering media significantly diminish contrast-to-noise ratio (CNR) of a target signal, leading to a great decline in image quality.[8–12] Nonetheless, an increased need for high-fidelity object reconstruction necessitates the attention of researchers toward scattering imaging. Some methods have been developed for CCD-based scattering imaging, e.g., memory effect,[13–17] wavefront shaping,[18–20] and measurement matrix.[21–23] However, random distribution of scattering media has a diverse impact on each detection pixel, still making optical imaging challenging as each pixel is differently affected.

Recently, optical imaging through scattering media with single-pixel detection is further developed and applied due to its high sensitivity and high CNR compared to 2D sensor-based imaging.[24–27] Among them, ghost imaging (GI) has become a promising optical technique that exploits object information acquired by a single-pixel detector, conferring inherent advantages in imaging through scattering media. A series of illumination patterns are employed to encode object information. The collected single-pixel light intensities are a one-dimensional (1D) signal, and correlation algorithms have been devised to extract the object from the acquired 1D signal.[28–36] Although GI has proven to be effective in scattering environments, there are still several inherent limitations. The GI was focused on assessing its viability and characteristics in static scattering scenarios.[37,38] However, dynamic and complex scattering phenomena (e.g., dynamic and turbid water) induce nonlinear effects, which bring a great challenge for ghost reconstruction due to an intricate interplay of scattering effect and dynamic nature.[39] Some studies were reported to enhance the quality of the recovered ghost images in dynamic scattering environments.[40–46] Xiao

et al.[45] reported a temporal correction (TC) method and introduced a temporally corrected pattern before each illumination pattern to solve the scattering problem. Although the TC method is effective for handling dynamic and complex scattering, it is accompanied by dramatically increased data acquisition time. Peng *et al.*[46] reported a learning-based correction with Gaussian constraints. However, deep learning method depends on the training dataset, and could be limited in real-world scenarios. It cannot satisfy a broad applicability. Therefore, an imperative lies in developing a method with general applicability and low complexity.

In this Letter, we report a correction algorithm based on an adaptive moving average (AMA) model for high-resolution and high-quality GI through dynamic and complex scattering media. The developed AMA model demonstrates aptitude in overcoming the challenges associated with dynamic scattering while maintaining computational efficiency and temporal expediency. From a statistical perspective, we propose to use a moving average model to estimate dynamic scaling factors caused by dynamic and complex scattering media. The AMA correction modality discerns an optimal time window predicated upon the mercurial trajectory of the realizations. The adaptive strategy augments its precision in counteracting the perturbations induced by dynamic and complex scattering media. When the influence of dynamic scattering media is corrected, corrected realizations can be further used with other algorithms to enhance reconstruction quality. High robustness is confirmed via theoretical derivations and experimental verifications, thereby realizing high-resolution ghost reconstruction in dynamic and complex scenes. Central to our proposition is the deployment of a moving average, which is instrumental in both the estimation and correction of dynamic scaling factors in an optical channel. When confronted with environments punctuated by intricate dynamics and pronounced scattering phenomena, it is experimentally verified that the proposed method outperforms other GI methods. The proposed method establishes a framework that transcends conventional understanding of GI from a statistical standpoint, providing a perspective for GI reconstruction in scattering environments, especially dynamic and complex scattering media.

A model is constructed based on the introduced obstruction of dynamic scattering media in GI. A series of illumination patterns $H_i(x, y)$ are sequentially multiplied by the projection function of a target object $O(x, y)$. Then, light intensities B_i ($i = 1, 2, 3, \ldots, M$) are collected by a single-pixel bucket detector, where M denotes the total number of realizations. The measurement vector in free space without scattering media can be described by

$$B_i = \int\int H_i(x, y)O(x, y)dxdy. \tag{1}$$

A schematic process is shown in Fig. 1(a). The single-pixel intensity measurements can be considered as a time series (a vector). When scattering media exist in the wave propagation path, the measurement vector can be described by

$$B_i' = k_i \int\int H_i(x, y)O(x, y)dxdy, \tag{2}$$

where B_i' denotes a collected light intensity in complex and dynamic scattering media corresponding to the ith illumination pattern, and k_i ($i = 1, 2, 3, \ldots, M$) denotes a scaling factor induced by scattering media. It can be seen in Eq. (2) that the dynamic scattering environment in GI could induce a different scaling factor in each realization, as shown in Fig. 1(b). In a static scattering environment, the values k_i can be assumed to be the same, and in a dynamic and complex scattering environment the values k_i could be nonlinearly changed. A relationship between the realizations in free space without scattering media and those in dynamic scattering media can be described by

$$B_i' = k_i B_i. \tag{3}$$

In Eq. (3), single-pixel light intensities are severely distorted in dynamic scattering media, and object wavefront cannot be reconstructed. It is desirable to eliminate the effect of dynamic scaling factors in GI through dynamic and complex scattering media.

Regarding the entire data acquisition process in GI, note that the single-pixel detection is linked to the illumination patterns. Random amplitude-only patterns are sequentially loaded onto a spatial light modulator (SLM), and the single-pixel intensity measurement is a time series. Due to the influence of dynamic scaling factors, single-pixel intensity measurements are distorted. To solve this problem, the moving average model is introduced to predict the trend of dynamic scattering factors in GI through dynamic and complex scattering media.

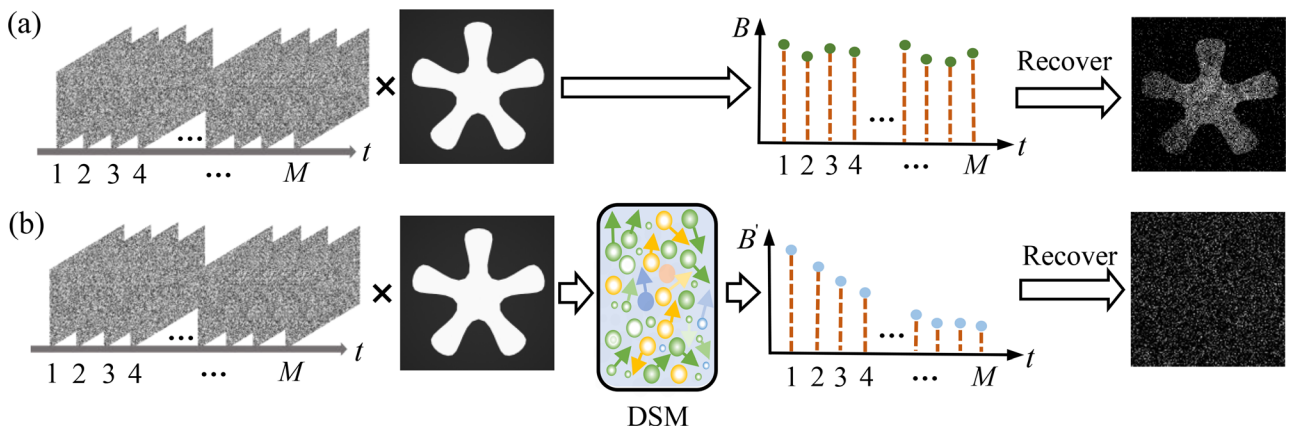

FIG. 1. Schematic of computational GI. (a) In free space without scattering media and (b) through dynamic and complex scattering media. DSM: Dynamic scattering media.

Using the designed moving average model, a correction of single-pixel intensity measurements can be described by

$$\hat{B}_i' = \frac{1}{L}\sum_{r=0}^{r=L-1} B_{i+r}' = \frac{1}{L}\sum_{r=0}^{r=L-1} k_{i+r}B_{i+r}, \tag{4}$$

where $\hat{B}_i'$ denotes the ith estimation of the realizations to characterize the trend of dynamic scaling factors, B' denotes single-pixel light intensities (i.e., realizations) collected in dynamic and complex scattering media, B denotes the collected single-pixel light intensities in free space without scattering media, i denotes the time index, and L denotes a time window length in the moving average model. Since the time interval to display adjacent illumination patterns is short in the selected window, dynamic scattering factors could be assumed not to have a change. Then, we have

$$k_i \approx k_{i+1} \approx \cdots \approx k_{i+L-2} \approx k_{i+L-1}. \tag{5}$$

Equation (4) can be rewritten as

$$\hat{B}_i' = \frac{1}{L}\sum_{r=0}^{r=L-1} B_{i+r}' \approx k_i \frac{1}{L}\sum_{r=0}^{r=L-1} B_{i+r} = k_i\bar{B}_L, \tag{6}$$

where $\bar{B}_L$ denotes a mean value of measured data in the time window. With the estimation, corrected realizations can be described by

$$\frac{B_i'}{\hat{B}_i'} \approx \frac{B_i'}{k_i\bar{B}_L} = \frac{k_iB_i}{k_i\bar{B}_L} = \frac{1}{\bar{B}_L}B_i. \tag{7}$$

As found in previous work,[47] using a series of random patterns to sequentially illuminate an object in GI, the distribution of collected light intensities obeys Gaussian. $\bar{B}_L$ can be considered to be a constant (see supplementary material, Note 1 for derivations). A symbol ρ is applied to replace $\bar{B}$ in Eq. (7), and we have

$$\frac{1}{\bar{B}_L} = \frac{1}{\rho}. \tag{8}$$

Therefore, Eq. (7) can be rewritten as

$$\frac{B_i'}{\hat{B}_i'} \approx \frac{1}{\bar{B}_L}B_i = \frac{1}{\rho}B_i. \tag{9}$$

In Eq. (9), dynamic scaling factors are effectively corrected using the moving average model. Then, ghost reconstruction in dynamic and complex scattering environments can be described by

$$\begin{aligned}\hat{O}(x,y) &= \left\langle \left(\frac{B_i'}{\hat{B}_i'} - \left\langle\frac{B_i'}{\hat{B}_i'}\right\rangle\right)[H_i(x,y) - \langle H_i(x,y)\rangle]\right\rangle \\ &= \left\langle \left(\frac{1}{\rho}B_i - \left\langle\frac{1}{\rho}B_i\right\rangle\right)[H_i(x,y) - \langle H_i(x,y)\rangle]\right\rangle \\ &\propto \langle (B_i - \langle B_i\rangle)[H_i(x,y) - \langle H_i(x,y)\rangle]\rangle,\end{aligned} \tag{10}$$

where $\hat{O}(x,y)$ denotes a reconstructed ghost image and $\langle\ \rangle$ denotes an ensemble average. In Eq. (10), the constant does not affect ghost reconstruction, and can be well processed by using a normalization operation.

Nonetheless, it is crucial to acknowledge that in real-world complex environments, solely relying on a fixed window moving average model could not suffice to overcome the challenges. Instances, such as unexpected environmental disruptions, accelerated water flow, or an abrupt presence of sludge, necessitate more comprehensive approaches. The AMA[48,49] was designed to consider volatility or noise of the measurement data, and seeks to identify and adapt to data change using AMA indicators. The indicators show the relative movement speed of single-pixel measurement data from one illumination pattern to another in GI. When fluctuations in the measured data are identified, the indicator adapts to its tracking mechanism and offers a reliable estimation of variations in the moving average. An efficiency ratio α is the key indicator utilized in the AMA correction algorithm, quantifying the variation of the realizations as follows:

$$\alpha_i = \frac{|B_i' - B_{i-n}'|}{\sum_{m=1}^{n}|B_i' - B_{i-m}'|}, \tag{11}$$

where the numerator denotes an n-measurements change, the denominator denotes a sum of the absolute value of every measurement change, and i starts from $n+1$. It is recommended[49] to set n as 10. The values α are in a range of [0, 1]. When there are substantial fluctuations in the realizations, α tends to be close to 1. When the measurements show a slight change, α is more likely to approach 0. The subsequent step in the estimation of AMA is the average itself. A recursive form of the weighted moving average is employed here, and the AMA can be described by

$$\begin{aligned}\left(\hat{B}_i'\right)_{AMA} &= \left(\hat{B}_{i-1}'\right)_{AMA} + c_i\left[B_i' - \left(\hat{B}_{i-1}'\right)_{AMA}\right] \quad (i > n), \\ \left(\hat{B}_i'\right)_{AMA} &= B_i' \quad (i \le n),\end{aligned} \tag{12}$$

where $(\hat{B}_i')_{AMA}$ denotes the ith current value of AMA estimation, $(\hat{B}_{i-1}')_{AMA}$ denotes the value of AMA in a previous window, and c_i denotes a smoothing factor at the ith estimated value. Incorporating the efficiency ratio, the factor is calculated by

$$c_i = [\alpha_i(F - S) + S]^2, \tag{13}$$

where F and S, respectively, denote "fastest" and "slowest" which correspond to two different lengths of moving average, respectively, described by

$$F = \frac{2}{k_f + 1}, \tag{14}$$

$$S = \frac{2}{k_s + 1}, \tag{15}$$

where k_f and k_s denote the number of measurements in the fastest and slowest applicable moving average, respectively. The recommended values[49] of k_f and k_s are initially set as 2 and 30, respectively. The AMA correction model integrates efficiency ratio α and the scaled weighting factor c to enhance the moving average estimation. After the corrected realizations are obtained, a reconstructed ghost image $\hat{O}(x,y)$ can be obtained in Eq. (10). The process is schematically shown in Fig. 2. The proposed method can provide a basis to be used with other algorithms to enhance reconstruction quality (see details in supplementary material, Note 2).

To verify the proposed AMA correction method, a series of optical experiments are conducted in GI through dynamic and complex

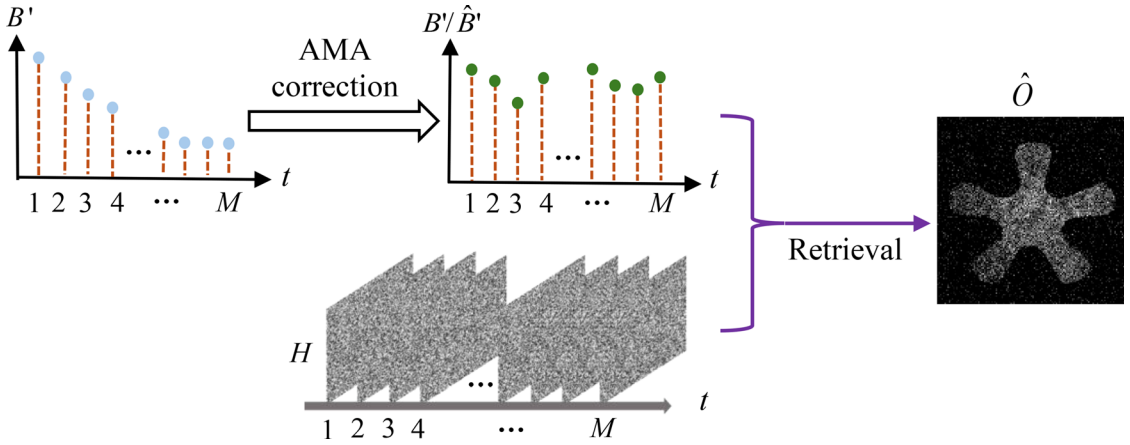

FIG. 2. A schematic of AMA correction. B': the realizations in complex and dynamic scattering media; $B'/\hat{B}'$: the AMA-corrected realizations; H: illumination patterns; and $\hat{O}$: a reconstructed ghost image.

scattering media. A schematic experimental setup is shown in Fig. 3(a). Here, the USAF 1951 resolution target is used as an object. A dynamic and highly strong scattering medium is established, when 20-ml skimmed milk dissolves in 1000-ml water to be continuously dropped into a water tank. Then, a stirrer with a speed of 600.0 revolutions per minute (rpm) is used to keep stirring in the data acquisition process (see details in supplementary material, Note 3). Without complex and dynamic scattering, a reconstructed ghost image is shown in Fig. 3(b). It is demonstrated that traditional GI can be applied to reconstruct clear target images in free space without scattering media.

In a dynamic and complex scattering environment, GI fails to recover any object information, as shown in Fig. 3(c). Although 40 000 realizations are used, object information still cannot be observed. The dynamic and complex scattering environment leads to wavefront distortion in the optical channel. Experimental results indicate that without any correction, GI framework is inadequate and unable to recover effective information about the object. When the proposed method is applied to correct dynamic scaling factors, a reconstructed ghost image is shown in Fig. 3(d). A high-resolution ghost image is reconstructed, and the image quality is close to that obtained in free space without scattering media. The finest structure resolved is group 2 element 6 of

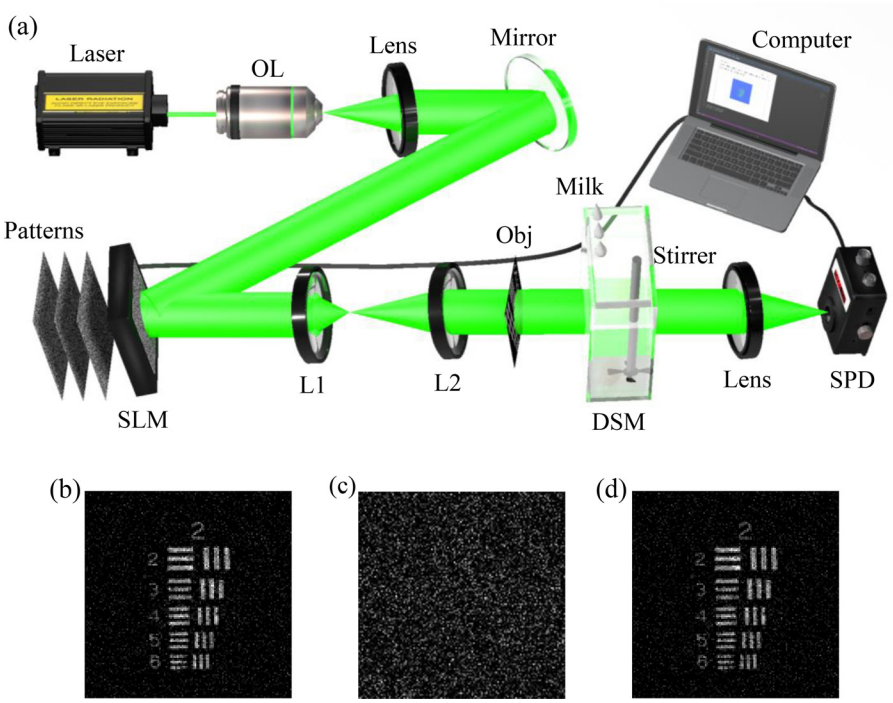

FIG. 3. (a) Schematic of an experimental setup. OL: objective lens; SLM: spatial light modulator; L1 and L2: 4f lens system; Obj: object; DSM: dynamic scattering media; SPD: single-pixel bucket detector. (b) A recovered ghost image using the traditional GI reconstruction method in free space without scattering media, (c) a recovered ghost image using the traditional GI reconstruction method in complex, dynamic, and highly strong scattering media, and (d) a reconstructed ghost image using the proposed method in complex, dynamic, and highly strong scattering media.

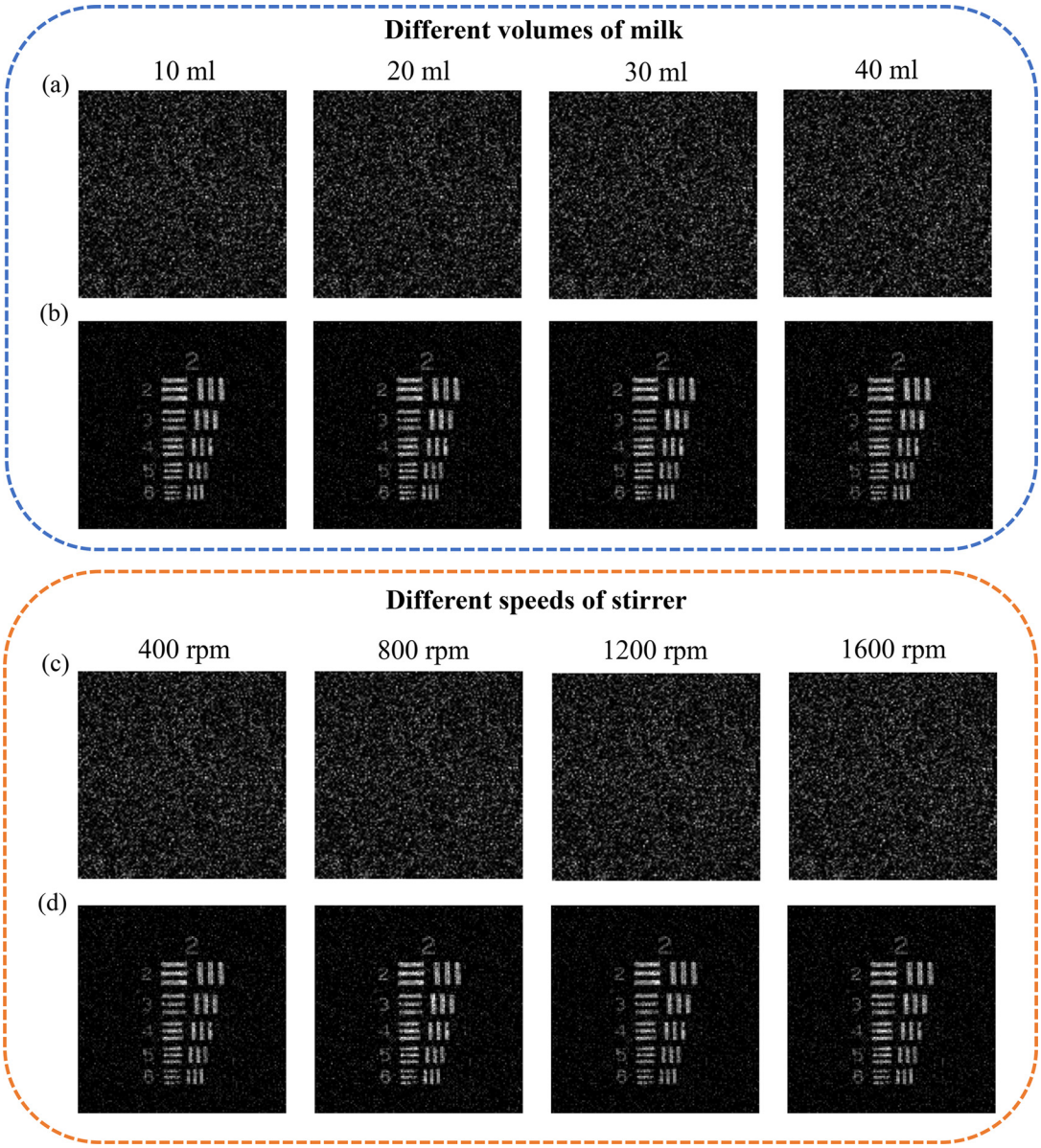

FIG. 4. The reconstructed ghost images (a) using the traditional GI method and (b) using the proposed AMA correction method with GI reconstruction when 10, 20, 30, and 40 ml of milk mixed with 1000-ml clean water is dropped into a water tank, respectively. The reconstructed ghost images (c) using the traditional GI method and (d) using the proposed AMA correction method with GI reconstruction when the speed of the stirrer is from 400 to 1600 rpm with an interval step of 400 rpm, respectively.

the USAF 1951 resolution target, and a spatial resolution of 140.31 μm is achieved. The comparison in Fig. 3 demonstrates superiority of the proposed method.

To illustrate the robustness, different volumes of milk are tested. The typically reconstructed ghost images are shown in Figs. 4(a) and 4(b), when 10, 20, 30, and 40 ml of milk mixed with 1000-ml water is, respectively, dropped into a water tank (see details in supplementary material, Note 4). Figure 4(a) shows the reconstructed ghost images using traditional GI. It is demonstrated that traditional GI has an inherent drawback regarding ghost reconstruction in dynamic and complex scattering media, and fails to recover any effective information about the object. When the proposed AMA correction algorithm is applied to rectify dynamic scaling factors, high-resolution ghost images are reconstructed as shown in Fig. 4(b).

Then, different speeds of the stirrer are tested when 20-ml milk is also used. The typically recovered ghost images are shown in Figs. 4(c) and 4(d) (see details in supplementary material, Note 4). Figure 4(c) shows the reconstructed ghost images using traditional GI. The experimental results demonstrate that the traditional GI method fails to recover the transmitted information in a dynamic and complex

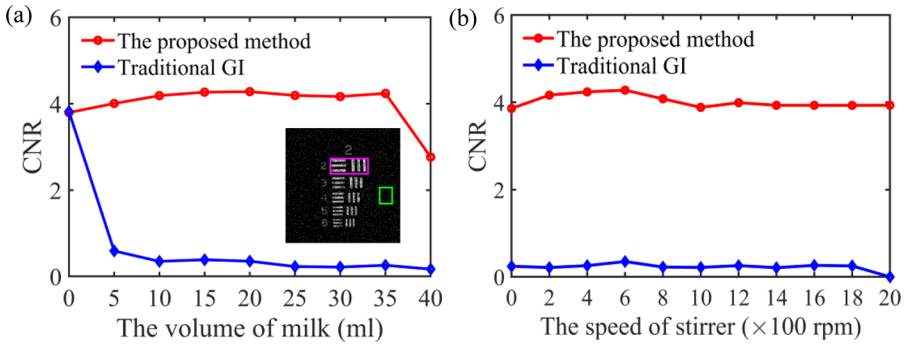

FIG. 5. (a) A relationship between the different volumes of milk and CNR values of the recovered ghost images (a fixed stirring speed of 600.0 rpm), and (b) a relationship between different speeds of stirrer and CNR values of the recovered ghost images (a fixed milk volume of 20.0 ml). The feature part contains only the bars inside the magenta box, and the background part is inside the green box.

scattering environment. Figure 4(d) shows experimental results obtained by using the proposed AMA correction method. The impact caused by dynamic and complex scattering environments is eliminated, and high-resolution ghost reconstruction is realized by using the proposed method.

Quantitative evaluation of the reconstructed ghost images is also conducted by calculating CNR (see definitions in supplementary material, Note 5). Figure 5(a) shows CNR values of the reconstructed ghost images using traditional GI and the proposed method, when different volumes of skimmed milk are used. When no milk is added into the water tank, the traditional GI algorithm can be used to recover object information and achieves a CNR value of 3.8. However, an increasing volume of milk added into the water tank exacerbates the presence of a scattering medium, and distorts the optical waves propagating in the optical channel. Consequently, traditional GI leads to a substantial decrease in CNR values. By using the proposed AMA correction method, CNR values of the reconstructed ghost images can reach a high level, when the volume of milk ranges from 0 to 35 ml. When the volume of milk reaches 40 ml, effective object information can still be recovered, as shown in Fig. 4(b).

Figure 5(b) shows CNR values of the reconstructed ghost images using traditional GI and the proposed method, when different speeds of the stirrer are used. For different speeds of the stirrer, CNR values of the reconstructed ghost images using the proposed AMA correction method are stable at a high level. In contrast, CNR values obtained by using the traditional GI method are always close to 0. The experimental results corroborate ineffectiveness of the traditional GI methods in complex and dynamic scattering environments, and feasibility and effectiveness of the proposed method are illustrated in recovering high-resolution ghost images in complex and dynamic scattering media.

In addition, another six samples are further tested to verify the proposed method in complex and dynamic scattering media (see supplementary material, Note 6 for details). The results show the feasibility of the proposed method. The proposed method can provide a basis to be used with other algorithms to enhance reconstruction quality (see supplementary material, Note 7 for details). It is demonstrated that the proposed AMA correction method provides a strong basis to be flexibly used in GI through dynamic and complex scattering media.

In conclusion, we have reported an AMA correction algorithm to reconstruct high-resolution ghost images by correcting a series of scaling factors physically induced by dynamic and complex scattering media in GI. The AMA correction algorithm can effectively eliminate the influence of dynamic scattering effect, and scaling factors can be estimated accurately using a moving average model. The AMA correction algorithm is realized by incorporating an efficacious ratio, enabling the heightened adaptability to dynamically environmental transitions. The UNN-enhanced algorithm is employed to further improve ghost reconstruction. The attributes of the proposed method encompass broad adaptability, system simplicity, and high robustness, and the proposed method offers a perspective to realize high-resolution and high-quality imaging through dynamic and complex scattering media.

See the supplementary material for the methods in detail and more experimental results.

This work was supported by the Hong Kong Research Grants Council (Nos. 15224921 and 15223522) and The Hong Kong Polytechnic University (Nos. 1-BD4Q and 1-WZ4M). The authors would like to thank Yin Xiao for an arrangement of the experimental setup.

AUTHOR DECLARATIONS

Conflict of Interest

The authors have no conflicts to disclose.

Author Contributions

Qian Song: Conceptualization (lead); Data curation (lead); Investigation (lead); Writing – original draft (lead). **Qing Huo Liu:** Formal analysis (lead); Supervision (lead); Writing – review & editing (lead). **Wen Chen:** Conceptualization (lead); Formal analysis (lead); Methodology (lead); Supervision (lead); Writing – review & editing (lead).

DATA AVAILABILITY

The data that support the findings of this study are available from the corresponding authors upon reasonable request.

REFERENCES

[1]J. S. Jaffe, K. D. Moore, J. McLean, and M. P. Strand, Oceanography **14**, 64 (2001).
[2]K. O. Amer, M. Elbouz, A. Alfalou, C. Brosseau, and J. Hajjami, Opt. Express **27**, 621 (2019).

[3]L. K. Choi, J. You, and A. C. Bovik, IEEE Trans. Image Process. **24**, 3888 (2015).
[4]H. Shi, G. Shen, H. Qi, Q. Zhan, H. Pan, Z. Li, and G. Wu, Opt. Express **30**, 12061 (2022).
[5]V. Ntziachristos, Nat. Methods **7**, 603 (2010).
[6]W. R. Zipfel, R. M. Williams, and W. W. Webb, Nat. Biotechnol. **21**, 1369 (2003).
[7]N. G. Horton, K. Wang, D. Kobat, C. G. Clark, F. W. Wise, C. B. Schaffer, and C. Xu, Nat. Photonics **7**, 205 (2013).
[8]J. Bertolotti, E. G. Van Putten, C. Blum, A. Lagendijk, W. L. Vos, and A. P. Mosk, Nature **491**, 232 (2012).
[9]S. Kang, S. Jeong, W. Choi, H. Ko, T. D. Yang, J. H. Joo, J. S. Lee, Y. S. Lim, Q. H. Park, and W. Choi, Nat. Photonics **9**, 253 (2015).
[10]S. Yoon, M. Kim, M. Jang, Y. Choi, W. Choi, S. Kang, and W. Choi, Nat. Rev. Phys. **2**, 141 (2020).
[11]J. Bertolotti and O. Katz, Nat. Phys. **18**, 1008 (2022).
[12]*Waves and Imaging through Complex Media*, edited by P. Sebbah (Springer Science & Business Media, France, 2001).
[13]O. Katz, P. Heidmann, M. Fink, and S. Gigan, Nat. Photonics **8**, 784 (2014).
[14]H. Yilmaz, E. G. van Putten, J. Bertolotti, A. Lagendijk, W. L. Vos, and A. P. Mosk, Optica **2**, 424 (2015).
[15]T. Zhang, X. Wang, W. Zhao, A. P. Zhai, C. Dang, and D. Wang, Adv. Photonics Res. **4**, 2300100 (2023).
[16]B. Hwang, T. Woo, C. Ahn, and J. H. Park, Laser Photonics Rev. **17**, 2200673 (2023).
[17]S. Li, S. A. R. Horsley, T. Tyc, T. Čižmár, and D. B. Phillips, Nat. Commun. **12**, 3751 (2021).
[18]A. P. Mosk, A. Lagendijk, G. Lerosey, and M. Fink, Nat. Photonics **6**, 283 (2012).
[19]M. Nixon, O. Katz, E. Small, Y. Bromberg, A. A. Friesem, Y. Silberberg, and N. Davidson, Nat. Photonics **7**, 919 (2013).
[20]R. Horstmeyer, H. Ruan, and C. Yang, Nat. Photonics **9**, 563 (2015).
[21]M. Mounaix, H. B. de Aguiar, and S. Gigan, Optica **4**, 1289 (2017).
[22]W. Fan, Z. Chen, V. V. Yakovlev, and J. Pu, Laser Photonics Rev. **15**, 2000376 (2021).
[23]A. Boniface, J. Dong, and S. Gigan, Nat. Commun. **11**, 6154 (2020).
[24]M. P. Edgar, G. M. Gibson, and M. J. Padgett, Nat. Photonics **13**, 13 (2019).
[25]D. Huyan, N. Lagrosas, and T. Shiina, APL Photonics **7**, 086104 (2022).
[26]W. Gong and S. Han, Opt. Lett. **36**, 394 (2011).
[27]L. X. Lin, J. Cao, D. Zhou, and Q. Hao, Opt. Commun. **529**, 129083 (2023).
[28]J. H. Shapiro, Phys. Rev. A **78**, 061802 (2008).
[29]O. Katz, Y. Bromberg, and Y. Silberberg, Appl. Phys. Lett. **95**, 131110 (2009).
[30]P. A. Moreau, E. Toninelli, T. Gregory, and M. J. Padgett, Laser Photonics Rev. **12**, 1700143 (2018).
[31]B. Sun, S. S. Welsh, M. P. Edgar, J. H. Shapiro, and M. J. Padgett, Opt. Express **20**, 16892 (2012).
[32]Z. Sun, F. Tuitje, and C. Spielmann, J. Microsc. **284**, 3 (2021).
[33]W. Yang, D. F. Shi, K. Han, Z. Guo, Y. Chen, J. Huang, H. Ling, and Y. Wang, Opt. Lett. **47**, 3123 (2022).
[34]F. Ferri, D. Magatti, L. A. Lugiato, and A. Gatti, Phys. Rev. Lett. **104**, 253603 (2010).
[35]Y. H. Zhai, X. H. Chen, D. Zhang, and L. A. Wu, Phys. Rev. A **72**, 043805 (2005).
[36]Y. Bromberg, O. Katz, and Y. Silberberg, Phys. Rev. A **79**, 053840 (2009).
[37]M. Bina, D. Magatti, M. Molteni, A. Gatti, L. A. Lugiato, and F. Ferri, Phys. Rev. Lett. **110**, 083901 (2013).
[38]F. Li, M. Zhao, Z. Tian, F. Willomitzer, and O. Cossairt, Opt. Express **28**, 17395 (2020).
[39]C. Stockbridge, Y. Lu, J. Moore, S. Hoffman, R. Paxman, K. Toussaint, and T. Bifano, Opt. Express **20**, 15086 (2012).
[40]Y. Sun, J. Shi, L. Sun, J. Fan, and G. Zeng, Opt. Express **27**, 16032 (2019).
[41]E. Tajahuerce, V. Durán, P. Clemente, E. Irles, F. Soldevila, P. Andrés, and J. Lancis, Opt. Express **22**, 16945 (2014).
[42]Z. Yu, L. Zhang, S. Yuan, X. Bai, Y. Wang, X. Chen, M. Sun, X. Li, Y. Liu, and X. Zhou, Opt. Eng. **62**, 021005 (2022).
[43]Y. Yu, M. Hou, C. Hou, Z. Shi, J. Zhao, and G. Cui, Sensors **23**, 9002 (2023).
[44]L. Zhou, Y. Xiao, and W. Chen, Appl. Phys. Lett. **123**, 011107 (2023).
[45]Y. Xiao, L. Zhou, and W. Chen, Opt. Lett. **47**, 3692 (2022).
[46]Y. Peng and W. Chen, Opt. Lett. **48**, 4480 (2023).
[47]H. Yang, S. Wu, H. B. Wang, D. Z. Cao, S. H. Zhang, J. Xiong, and K. Wang, Phys. Rev. A **98**, 053853 (2018).
[48]C. A. Ellis and S. A. Parbery, Res. Int. Bus. Finance **19**, 399 (2005).
[49]P. Kaufman, *Smarter Trading* (McGraw-Hill, New York, 1995).